ACS OMEGA

Article

Cite This: ACS Omega 2019, 4, 5356−5366

http://pubs.acs.org/journal/acsodf

Aggregation of Microtubule Binding Repeats of Tau Protein is Promoted by Cu^{2+}

Soha Ahmadi,[†,‡] Shaolong Zhu,[§,∥] Renu Sharma,[†] Bing Wu,[†,⊥] Ronald Soong,[†,‡] R. Dutta Majumdar,[†,#] Derek J. Wilson,[*,§,∥] Andre J. Simpson,[*,†,‡] and Heinz-Bernhard Kraatz[*,†,‡]

[†]Department of Physical and Environmental Science, University of Toronto Scarborough, 1265 Military Trail, Toronto, Ontario M1C 1A4, Canada

[‡]Department of Chemistry, University of Toronto, 80 St. George Street, Toronto, Ontario M5S 1A1, Canada

[§]Chemistry Department, York University, Toronto, Ontario M3J1P3, Canada

[∥]The Centre for Research in Mass Spectrometry, York University, 4700 Keele Street, Toronto, Ontario M3J1P3, Canada

Supporting Information

ABSTRACT: Understanding the factors that give rise to tau aggregation and reactive oxygen species (ROS) is the key aspect in Alzheimer's disease pathogenesis. Microtubule (MT) binding repeats of tau protein were suggested to play a critical role in tau aggregation. Here, we show that the interaction of Cu^{2+} with full-length MT binding repeats R1−R4 leads to the aggregation, and a Cys-based redox chemistry is critically involved in tau aggregation leading to disulfide-bridge dimerization of R2 and R3 and further aggregation into a fibrillar structure. Notably, ascorbate and glutathione, the most abundant antioxidants in neurons, cannot prevent the effect of Cu^{2+} on R2 and R3 aggregation. Detailed ESI-MS and NMR experiments demonstrate the interaction of Cu^{2+} with MT binding repeats. We show that redox activity of copper increases when bound to the MT repeats leading to ROS formation, which significantly contribute to cellular damage and neuron death. Results presented here provide new insights into the molecular mechanism of tau aggregation and ROS formation and suggest a new target domain for tau aggregation inhibitors.

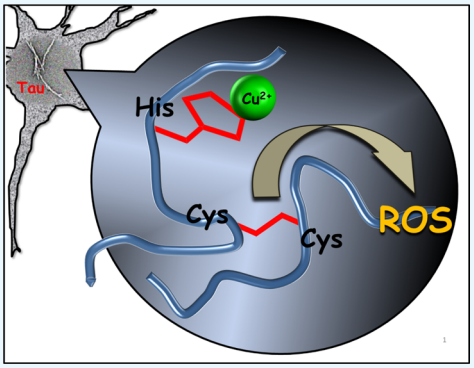

INTRODUCTION

Pathogenesis of Alzheimer's disease (AD) like other neurodegenerative diseases involves abnormal protein aggregation in the central nervous system. While aggregation of amyloid-β (Aβ) leads to the formation of extracellular amyloid plaques, aggregation of tau protein results in the formation of intracellular neurofibrillary tangles (NFTs).[1−4] Protein aggregation is a multistep process, which starts with abnormal protein conformational changes and continues by dimerization or oligomerization with subsequent formation of amyloid plaques or NFTs.[5−7] Experimental evidence suggests that not only amyloid plaques and NFTs are involved in neuronal death, but small toxic aggregates more likely contribute to the cell toxicity.[6−8] A number of factors can give rise to protein aggregation, including environmental stress and ageing.[3,6,7] Previous reports also showed that metals such as zinc, iron, and copper, which are essential for normal brain function, are unusually accumulated in the brain of AD patients.[9−11] Even though the concentrations of free metal ions are tightly controlled, metal dyshomeostasis under pathological conditions may lead to the enhancement of free metal ions in neurons.[9,11] In particular, copper, which is involved in many enzymatic activities in the brain, not only presents as a tightly bound cofactor but labile and mobile copper ions are also involved in neural activity.[12,13] Both mono- and divalent are essential for copper cofactor activity, in which reactive oxygen species (ROS) is generated through transition between two oxidation states of copper.[14,15] In a healthy condition, the $Cu^{+/2+}$ distribution is highly regulated by an efficient homeostatic mechanism in the brain, in addition to detoxification of ROS. In addition, while the predominant oxidation state in a healthy condition would presumably be Cu^{+} within neurons, dyshomeostasis and ROS formation may contribute to a considerable level of Cu^{2+}.[12,14−16] Also, this might certainly be of relevance in the later stages of the disease.

A study by Squitti et al. showed that the copper content of cerebrospinal fluid (CSF) in AD patients is higher than that for a healthy control, which may be related to the lability of serum copper that can be passed through the blood-brain barrier.[17] An increase in the level of peroxides and tau protein in CSF, which is confirmed by this study, may suggest a neurotoxic effect of copper.[17] In animal experiments, the neurotoxicity of

Received: December 21, 2018
Accepted: March 5, 2019
Published: March 15, 2019

DOI: 10.1021/acsomega.8b03595
ACS Omega 2019, 4, 5356−5366

copper was demonstrated by the addition of a trace amount of Cu^{2+} to the drinking water, which enhanced the animal's memory loss.[18,19] While there are a number of studies reporting the interaction of Cu^{2+} with tau and some of its fragment peptides,[20−25] the role of Cu^{2+} on tau aggregation is not well understood. Previous studies suggested that two hexapeptide motifs within R2 (^{275}VQIINK^{280}) and R3 (^{306}VQIVYK^{311}) are involved in the formation of paired helical filaments (PHFs).[26−29] More detailed cryo-electron microscopy studies by Fitzpatrick et al. and by Falcon et al. of PHFs demonstrate the presence of different tau isoforms within.[30,31] The presence of cysteine (Cys) in R2 and R3 (Scheme 1) is another feature that may contribute to aggregation by the formation of a disulfide bond. Experiments reported by others on tau peptide constructs which possess a Cys residue demonstrated the disulfide bond formation.[32,33] Furthermore, the potential for ROS generation due to the redox reaction of Cu^{2+} with Cys of tau protein has not been well studied. In this report, we provide unequivocal evidence of the interaction of Cu^{2+} with full-length microtubule (MT) binding repeats R1 (tau244-274), R2 (tau275-305), R3 (tau306-336), and R4 (tau337-368), which lead to the peptide aggregation and solid evidence for fibril formation and ROS generation for R2 and R3.

Scheme 1. (A) Schematic Representation of htau40 (2N4R) Isoform, Displaying the Major Domains Consisting of Project Domain, Proline-Rich Domain, and MT Binding Domain; (B) Amino Acid Sequence of MT Binding Repeats (R1, R2, R3, and R4)

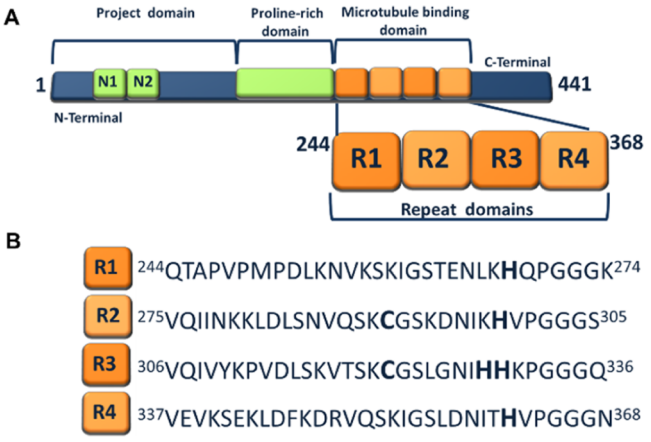

Tau, an MT-associated protein with six isoforms (Scheme S1), which is mainly expressed in neurons, is an intrinsically disordered protein, highly water-soluble and with low tendency to aggregate under normal physiological conditions.[1,4] Tau proteins are attached to the MTs through an MT- binding domain consisting of three or four MT binding repeats R1−R4 (Scheme S1).[1,4,34] The MT binding repeats not only play a critical role in MT assembly but also play a key role in the aggregation of the tau protein.[1,34] The formation of the disulfide bond due to the presence of cysteine in R2 and R3 may further implicate to the protein aggregation.[32,33] Because MT binding repeats are of such importance, we hypothesized that these motifs also play an essential role in copper-tau interaction, which may lead to the tau aggregation and ROS formation. Previous studies involving short 18-mer peptides of R1, R2, and R3 demonstrated that these peptides indeed interact with Cu^{2+}, giving rise to conformational changes.[20−22] Earlier works from our group reported on the interactions of Cu^{2+}, Zn^{2+}, and $Fe^{2/3+}$ with surface-bound htau39 (2N3R) (Scheme S1) using electrochemical techniques.[24,35] We demonstrated that conformational changes occur as a result of the interaction of htau39 with $Fe^{2/3+}$.[35] Our recent studies showed that the interaction of $Fe^{2/3+}$, Zn^{2+}, and Cu^{2+} with full-length htau40 leads to the protein aggregation. Furthermore, in

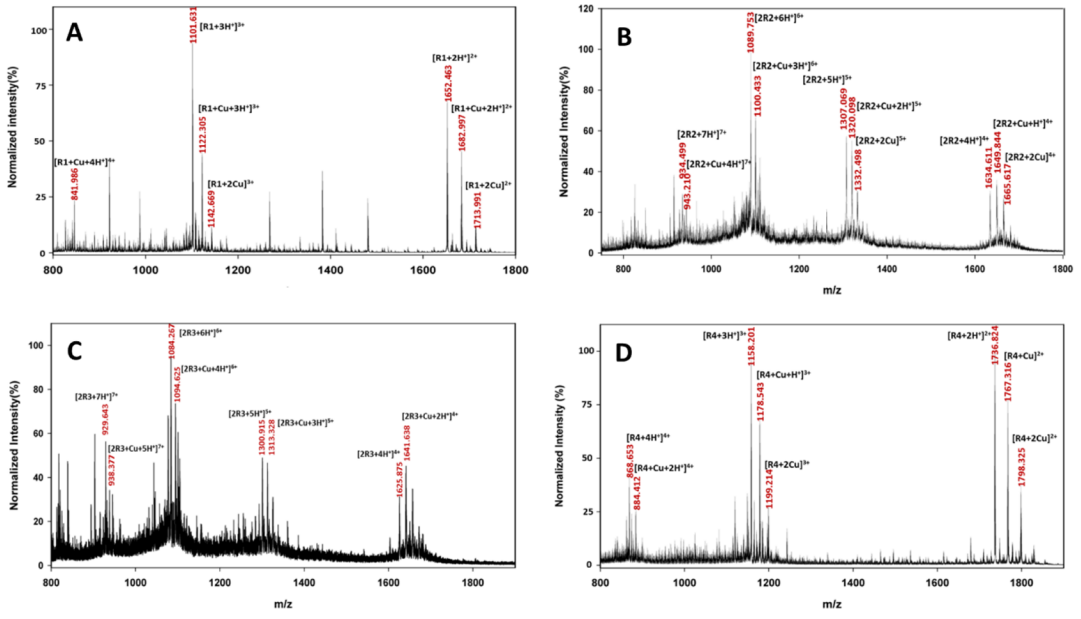

Figure 1. ESI-MS spectra (see Figures S1−S4 for details) of 70 μM MT binding repeats (A) R1, (B) R2, (C) R3, and (D) R4 after incubating in 140 μM Cu^{2+} solution (2:1 molar ratio of Cu/R) at 25 °C (pH 7.4) for 24 h. The ESI-MS results confirm the metalation of MT binding repeats. While mono- and dimetalation of R1 and R4 are observed, dimerization occurs upon interaction of Cu^{2+} with Cys-containing MT binding repeats R2 and R3. Metalation of R2 and R3 dimers are also confirmed by the ESI-MS spectrum.

DOI: 10.1021/acsomega.8b03595
ACS Omega 2019, 4, 5356−5366

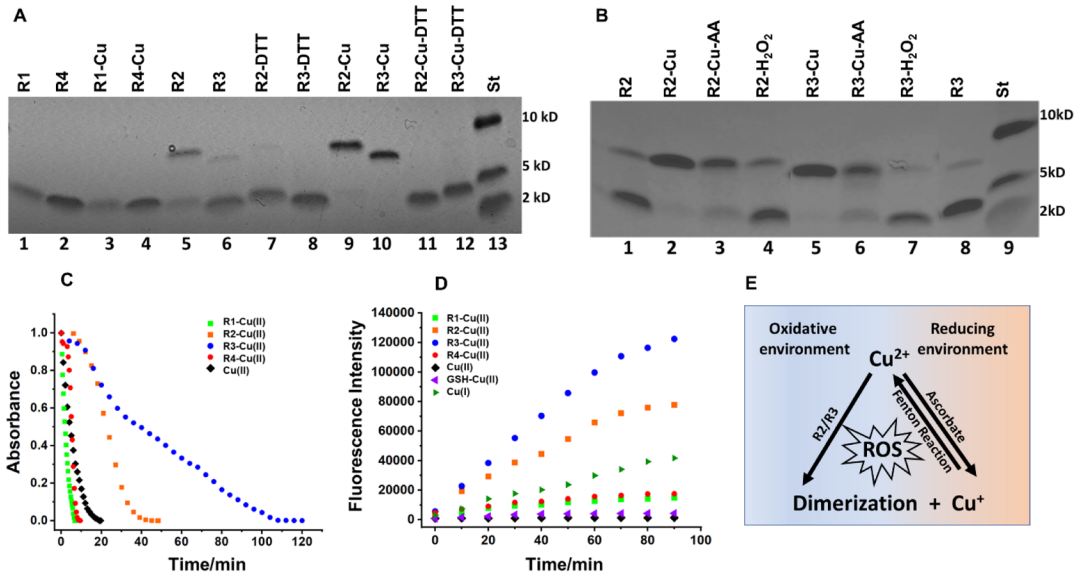

Figure 2. (A) Gel electrophoresis for MT binding repeats (R1−R4) with and without incubation in Cu^{2+} solution at 25 °C for 24 h (molar ratio 2:1 of Cu/R), which confirm the disulfide bond formation upon interaction of Cu^{2+} with R2 and R3. (1) R1, (2) R4, (3) R1−Cu, (4) R4−Cu, (5) R2, (6) R3, (7) R2−DTT, (8) R3−DTT, (9) R2−Cu, (10) R3−Cu, (11) R2−Cu−DTT, (12) R3−Cu−DTT, and (13) standard protein. (See the Supporting Information for the details) (B) gel electrophoresis for MT binding repeats R2 and R3 after being incubated at 25 °C for 24 h in (a) $CuCl_2$ at a molar ratio of 1:2 of R/Cu; (b) AA and $CuCl_2$ at a molar ratio of 1:20:2 of R/AA/Cu; (c) H_2O_2 at a molar ratio of 1:2 of R/H_2O_2. (1) R2, (2) R2(a), (3) R2(b), (4) R2(c), (5) R3(a), (6) R3(b), (7) R3(c), (8) R3, and (9) standard protein. These results show that Cu^{2+} play a key role in R2/R3 dimerization. (C) UV−visible study of 10 μM Cu^{2+} interaction with 5 μM R1 (green), R2 (orange), R3 (blue), and R4 (red) in the presence of 100 μM AA. A solution of Cu^{2+} (black) was monitored under the same conditions as the control sample. (D) Time-dependent experiment for monitoring the ROS formation after adding the 5 μM Cu^{2+} solution to the 5 μM R1 (light green), R2 (orange), R3 (blue), and R4 (red) solution using fluorescence intensity of DCF (523 nm) as a fluorescence probe. A solution of Cu^{2+} (black), GSH with Cu^{2+} (purple), and Cu^{+} (dark green) was monitored at same conditions as control samples. Interactions of Cu^{2+} with R2/R3 lead to the ROS formation as a consequence of disulfide bond formation. (E) Schematic representation of the proposed catalytic role of Cu^{2+} in the dimerization and ROS formation.

the case of redox-active metal ions, these interactions promote ROS formation.[36] However, there is still a lack of information about the interaction of Cu^{2+} with the full-length MT binding repeats R1, R2, R3, and R4, the ability of these peptides to aggregate in the presence of Cu^{2+}, and detailed studies of ROS formation.

In the present study, we explore the interaction of all four MT binding repeats R1−R4 of tau (htau40) with Cu^{2+} (Scheme 1B) by focusing on the chemistry aspect of these interactions. Given the possibility of redox activity of cysteine, we report on significant differences in chemical behavior, as well as in ROS formation and aggregation profile between R1−R4 and the cysteine-containing MT repeats R2/R3. In addition, while our current studies provide information about metal coordination to peptide fragments R1−R4, their reactivity with regard to ROS formation, and peptide aggregation, there are inherent limitations when working with the peptide fragment, as such studies may provide results that differ from those involving the entire protein.

RESULTS AND DISCUSSION

Interactions of Cu^{2+} with MT Binding Repeats Mediate the Dimerization in R2 and R3. Complexation of Cu^{2+} with all four MT binding repeats was confirmed by ESI-MS experiments (Figure 1); while for R1 and R4, metalation was observed leading to the formation of M + Cu and M + 2Cu adducts, for R2 and R3, ESI-MS results showed the presence of peptide dimers. The ESI-MS spectrum (Figures 1A and S1) depicts the mono- and dimetalation of R1, leading to the formation of multiple charged ions (+2, +3 and +4). Nevertheless, peaks of native R1 is predominant, and peaks related to the R1−Cu complex have appreciable intensities. Comparing intensities of R1−Cu complex peaks to those related to R1−2Cu suggests a two-step reaction (Scheme S2). The interaction of R4 with Cu^{2+} also results in the formation of R4−Cu and R4−2Cu complexes (Figures 1D and S4). Remarkably, the interactions of the Cys-containing repeats R2 and R3 with Cu^{2+} show a more complex chemistry and dimerization, which is one of the key features of this interaction, as confirmed by multiple charged 2M and 2M−Cu ions (+4, +5, +6, and +7) (Figures 1B,C, S2, and S3). Interestingly, there is no evidence for the formation of the M−Cu complex for R2 and R3 as previously reported for shorter R2/R3 tau peptides.[21,22] Instead, metal complexes identified are only related to R2 and R3 dimers. It should be mentioned that dimerization was not reported for the 18-mer R2 and R3 before.[21,22] The ESI-MS spectrum shows signals identified as the dimer of R2 at m/z of 934.50, 1089.75, 1307.07, and 1634.61 with charges of 7, 6, 5, and 4, respectively. Similarly, signals related to the dimerization of R3 are identified at m/z of 929.64, 1084.27, 1300.92, and 1625.88 with charges of 7, 6, 5, and 4, respectively. The dimerization is the result of the reactivity of R2 and R3 with Cu^{2+} as is confirmed by gel electrophoresis of R1−R4 in the presence of Cu^{2+} (Figure 2A).

As can be seen from Figure 2A, dimerization is observed for R2 and R3 (traces 9 and 10) in the presence of Cu^{2+} and is absent for R1 and R4 (traces 3 and 4). Some dimerization of peptides R2 and R3 occurs even in the absence of Cu^{2+} as indicated in Figure 2A (traces 5 and 6). However, in the presence of Cu^{2+}, all of R2 and R3 is converted to the

DOI: 10.1021/acsomega.8b03595
ACS Omega 2019, 4, 5356−5366

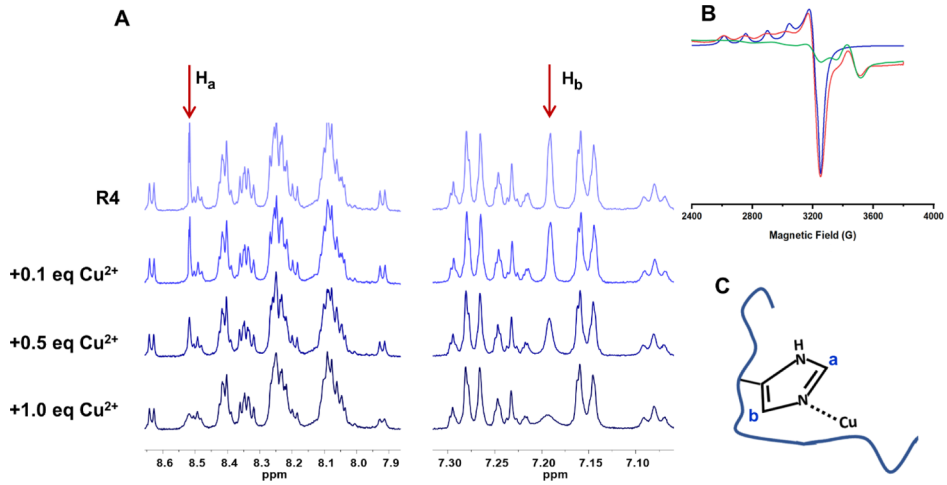

Figure 3. (A) Partial ^{1}H NMR spectra showing the aromatic region of R4 (2 mM of R4 at 25 °C at pH 7.4). Addition of Cu^{2+} to a solution of R4 and effects on the line broadening of the imidazole H. Note the line broadening of the H_a and H_b of the imidazole ring at 8.52 and 7.19 ppm, respectively, as a result of Cu^{2+} addition, clearly indicating the interaction of the His imidazole with the Cu^{2+} ion, as indicated in the schematic representation. (B) X-band EPR spectra of frozen solution of MT binding repeat R4 after incubating in Cu^{2+} solution at 25 °C (pH 7.4) with a molar ratio R/Cu of 1:2 (red), the simulation spectrum using EPRNMR software (blue). Cu^{2+} in phosphate buffer at pH 7.4 is provided as a control (green) (see the Supporting Information for the details). The results confirm that all R−Cu complexes have the same coordination; the coordination to the imidazole ring of His has been also confirmed by NMR. (C) Proposed scheme for the coordination environment of R−Cu complexes based on the EPR and NMR results.

corresponding dimer and no monomer was observed (Figure 2A, traces 9 and 10). It can be assumed that the thiol groups of cysteine residues present in R2 (Cys291) and R3 (Cys322) are involved in the oxidation to the respective disulfide bonds as indicated in Scheme S3A. Dimers disappeared (traces 11 and 12) after treatment with the dithiothreitol (DTT, as a reducing agent), which confirms the formation of dimers through the disulfide bond. Inter- and intramolecular disulfide bond formation due to redox activity of Cu^{2+} is a well-defined process; however, this is the first time that is reported for the MT binding repeats of tau protein, which leads to the dimerization. The disulfide bond in tau fragments can also be triggered by H_2O_2 as was shown by Walker et al.[37] In order to evaluate the impact of Cu^{2+}, we performed gel electrophoresis after incubating R2/R3 with H_2O_2 under the same condition as for Cu^{2+} (Figure 2B traces 4 and 7). The results show that the dimerization for R2/R3 in the presence of Cu^{2+} is more significant compared to H_2O_2, which suggest that Cu^{2+} complexation may play an important role in the disulfide bond formation (Figure 2B). We also examined the dimerization of R2/R3 in a reducing environment by performing gel electrophoresis for the solution of R2/R3 after incubating in a solution of Cu^{2+} and 10 mM ascorbic acid (AA) (1:20:2 molar ratio of R/AA/Cu^{2+}) to provide a reducing environment (Figure 2B, traces 3 and 6). Gel electrophoresis results confirm that the interaction of copper with R2/R3 in a reducing environment also leads to the R2/R3 dimerization.

We also performed a competitive study to evaluate the ability of ascorbate to reduce Cu^{2+} in the presence of MT binding repeats. Figure 2C shows the reduction of AA absorbance (262 nm) in the solution of MT binding repeats R1−R4 in the presence of Cu^{2+} (1:20:2 molar ratio of R/AA/Cu^{2+}). The time-dependent experiments show (Figures 2C and S5) that AA in the solution of R1 and R4 reduced as fast as the control sample without peptides, while the AA reduction in the solution of R2 and R3 took 40 and 100 min, respectively. These results indicate that R2 and R3 have more affinity to react with Cu^{2+} than AA, which suggests that AA cannot combat the Cu^{2+} reactivity even at very high concentration and explain the R2 and R3 dimerization in the presence of AA (Figure 2B). This observation more emphasizes the differences between Cys-containing MT repeats R2/R3 and R1−R4.

The redox process between Cu^{2+} and Cys results in the formation of a disulfide bond, while Cu^{+} is formed in the process (Scheme S3A). Presumably, Cu^{+} has the potential to be involved in reactions that lead to the formation of ROS.[38−40] Ząbek-Adamska et al. claimed that the Cu(II)−His_2 complex in the presence of cysteine produce ROS.[41] They proposed a cyclic mechanism in which the Cu(II)−His_2 complex binds to the Cys and while Cys oxidizes, Cu(I)−His_2 is formed. The Cu(I)−His_2 is able to be involved in Fenton reaction and producing ROS, in which Cu(II)−His_2 is generated again that is capable of oxidizing Cys.[41] Our observation reinforces the proposed mechanism because even low concentration of Cu^{2+} causes R2/R3 dimerization as the same extent that occurs in the presence of excess Cu^{2+}. Figure 2E illustrates a proposed catalytic role of Cu^{2+} in the dimerization, which may lead to the ROS formation.

ROS Formation upon Cu^{2+} Interactions. Oxidative damage is one of the key events in ageing that has been implicated in many diseases including AD, which is because of misregulation of ROS. In order to probe the formation of ROS upon interaction of Cu^{2+} with MT binding repeats, we examined changes of the fluorescence intensity of 2,7-dichlorofluorescein (DCF, as a fluorescence ROS probe) at 523 nm.[42,43] Figure 2D (Figure S6B,C) shows an increase in the fluorescence intensity when Cu^{2+} is added to solutions of R2 and R3 which reach a plateau after 100 min, while solutions of R1 and R4 in the presence of Cu^{2+} and DCF do not exhibit any appreciable increase of the fluorescence intensity (Figures 2D and S6A,D). The fluorescence intensity corresponds to the amount of ROS that is released because of the redox activity of the R−Cu complex. The fluorescence intensity of R2−Cu and

DOI: 10.1021/acsomega.8b03595
ACS Omega 2019, 4, 5356−5366

R3−Cu was higher compared to the R1−R4 complexes, allowing us to conclude that ROS formation is a consequence of disulfide bond formation, for which Cu^{+} is generated (Figures 2D and S6B,C).

Gaubert et al. showed that histidine decreases the redox potential of Cu^{2+}/Cu^{+}, which enhances the Fenton reaction.[44] We performed a surfaced-based electrochemical experiment to investigate the redox activity of R−Cu complexes. Our results show a decrease in the redox potential of Cu^{2+}/Cu^{+}, which are in line with Gaubert's results (Figures S7−S9 and Table S1). Based on these results, and because of the affinity of histidine to copper, we hypothesized that histidine is the putative binding site of Cu^{2+}.

Coordination Chemistry of R−Cu Complex. Next, detailed studies of the interaction of Cu^{2+} with R1−R4 by a series of NMR experiments were performed. Although there is an explicit difference between the interaction of R1−R4 and R2/R3 with Cu^{2+}, similarities in the amino acid sequence of these peptides suggest that they may have the same copper coordination as reported for the 18-mer R peptides.[20−22,45] We examined the hypothesis that the histidine residue is the potential binding site for the Cu^{2+} by assuming that Cu^{2+} remains paramagnetic in the peptide complex. Cu^{2+} coordination to the imidazole of His will result in paramagnetic contact shifts and will give rise to significant line broadening in the NMR spectra.[46,47] Given the paramagnetic nature of Cu^{2+}, coordination to the imidazole ring is expected to result in line broadening of the imidazole H, which is because of the interaction with the unpaired spin of d^9 Cu^{2+}, causing changes in the relaxation time. Figure 3A shows the ^{1}H NMR spectrum of R4, which depicts two sharp signals that are assigned to the protons H_a and H_b at 7.19 and 8.50 ppm. The assignments of the amino acid residues are based on previous reports.[20−22,25,29] In the absence of Cu^{2+}, the ^{1}H NMR spectra of all 4 peptides consisted of ^{1}H resonances that span almost the entire ^{1}H chemical shift range (Figures 3A and S10−S13). Based on their relatively narrow line shape, these peptides are likely undergoing isotropic motions that average out various undesirable line broadening interactions. As can be expected, the response to the addition of Cu^{2+} differs between the different MT binding repeats. This can be due to several factors, including peptide aggregation and paramagnetic relaxation. As shown in Figures S10 and S13, in the absence of the cysteine residue, the interaction of Cu^{2+} with R1 or R4 mainly occurred at the imidazole group of His. Furthermore, the relaxometry data (Figures S14 and S17) of R1 and R4 further support the results of the 1D ^{1}H NMR. In both peptides, the most prominent changes in both T_1 and T_2 occur in the aromatic region, while both T_1 and T_2 of the aliphatic region remain relatively similar regardless of the R/Cu^{2+} molar ratio. In the case of R2 and R3, an interaction still appears to take place at His as indicated by the broadening of this residue in both cases; however, the cysteine has a significant impact in the Cu^{2+} interaction (Figures S11 and S12). As concluded from the ESI-MS and gel electrophoresis results and based on the literature,[23,48,49] the thiol group in cysteine is prone to form a disulfide bond through the oxidative folding when an oxidizing agent like Cu^{2+} is introduced. As shown in Figures S11 and S12, the gradual disappearance of cysteine H2 and H3 peaks was found in both R2 and R3 after adding the Cu^{2+} solution, while a rather broad cysteine H3 (consistent with the disulfide unit) peak slowly appeared in their spectra. The corresponding NMR relaxometry (Figures S15 and S16) also shows a large reduction in both T_1 and T_2 values for R2 and R3 across the entire ^{1}H chemical shift range, compared to their noncysteine-containing counterparts (R1 and R4), in which only aromatic residues are predominantly affected by Cu^{2+}. The change in relaxation of essentially all protons in R2 and R3 indicates a drastic change in the overall protein rigidity and suggests that the peptides are undergoing aggregation (Figures S15 and S16). These observations further support the notion that the disulfide bond is formed by Cu^{2+} in R2 and R3.

In order to assess the copper coordination in the R−Cu complex, electron paramagnetic resonance (EPR) studies were carried out. Given the presence of a single unpaired electron in Cu^{2+}, EPR is a useful tool that provides information about the specific coordination environment. Figure 3B shows the EPR spectrum of the MT binding repeats R4 after incubating in Cu^{2+} solution for 24 h (see Figure S18 for the EPR spectrum of other R−Cu complexes). Our experiment showed, as reported before,[45] that the EPR signal for Cu^{2+} solution in phosphate buffer (pH 7.4) is negligible and does not interfere with the signal of the R−Cu complex (Figure 3B, green line). Simulation of the EPR spectrum gave a reasonable fit of the experimental data with the axial Cu^{2+} center (Figure 3B, blue line). This result indicates that the copper coordination environment is the same for all MT binding repeats, which means that copper complexation is an independent reaction from the dimerization for R2 and R3. This observation also rejects the hypothesis of the formation of the copper bridge in R2 and R3 dimers (Scheme S3B) and further supports the formation of disulfide bond during the dimerization (Scheme S3A). The simulation gave the value of $g_{\|} = 2.361$ and $g_{\perp} = 2.077$, and hyperfine splitting $A_{\|} = 165$ G and $A_{\perp}$ equal to 9 G. Based on the Peisach−Blumberg classification,[50−53] the Cu^{2+} is located within a type 2 coordination geometry. Potential ligating sites include the His imidazole N, backbone amides N or O as well as other oxygen-based ligating sites, including potential influence of solvation. A number of Cu-peptides have been structurally characterized allowing a detailed analysis of the Cu-coordination environment.[51−54] The EPR results further support the coordination of the imidazole ring of His to Cu^{2+}, as indicated in Figure 3C. The involvement of the peptide backbone in coordination to Cu^{2+} is well known and a number of structurally well-characterized examples have been reported in the literature.[38,55−58] Others noted that the coordination environment in some Cu-peptide complexes is influenced by dynamic solvation.[59] For the shorter 18-mer peptides, Shin and Saxena[45] also suggested the His residue as a putative binding site for the pseudo-repeats. However, specific coordination environments may vary significantly as Sakaguchi and Addison[60] showed that the $g_{\|}/A_{\|}$ values can be used to evaluate the tetrahedral distortion. Lower $A_{\|}$ and higher $g_{\|}$ compared to what was reported for pseudo-repeats[45] suggests a tetrahedral distortion of square planar geometry.[60]

Influence of Cu^{2+} on the Aggregation of MT Binding Repeats. Importantly, there are significant differences in the ability of R1−R4 to aggregate in the presence of Cu^{2+}. Results presented here show that disulfide bond formation for R2 and R3 results in the formation of dimers (Figures 1 and 2A,B). Peptide dimerization is the early stage of the aggregation. ESI-IMS-MS results allow us to evaluate structural changes as a result of the interaction of R1−R4 with Cu^{2+}. The DriftScope plot (Figure S19) shows the distribution of species based on their m/z and drift time, which is determined by the collisional cross section (CCS) of the species. Comparing the drift time

DOI: 10.1021/acsomega.8b03595
ACS Omega 2019, 4, 5356−5366

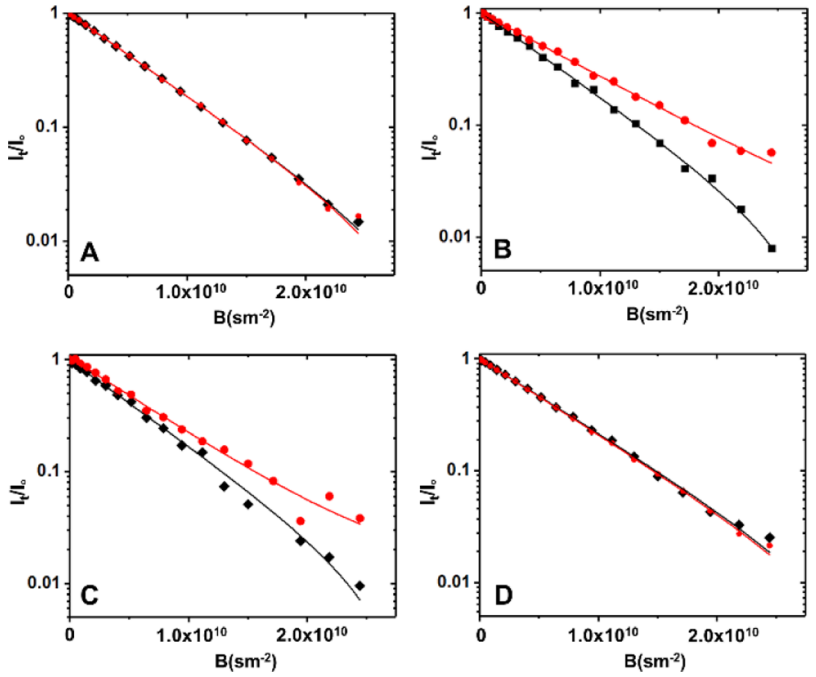

Figure 4. ^{1}H NMR diffusometry analyses for 2 mM MT binding repeat (A) R1, (B) R2, (C) R3, and (D) R4 before (black fitting curve) and after incubating in 2 mM Cu^{2+} (red fitting curve) solution at 25 °C (pH 7.4). The diffusion coefficient did not show significant changes for R1 (D = 1.70 × 10^{-10} m^2/s) and R1−Cu (D = 1.73 × 10^{-10} m^2/s). The same results were obtained for R4 (D = 1.65 × 10^{-10} m^2/s) and R4−Cu (D = 1.69 × 10^{-10} m^2/s). However, there was considerable decrease in the diffusion coefficient when Cu^{2+} is added to R2 (D_{R2} = 1.82 × 10^{-10} m^2/s, D_{R2-Cu} = 1.43 × 10^{-10} m^2/s) and R3 (D_{R3} = 1.74 × 10^{-10} m^2/s, D_{R3-Cu} = 1.20 × 10^{-10} m^2/s), which indicates that Cu^{2+} triggers the aggregation in R2 and R3.

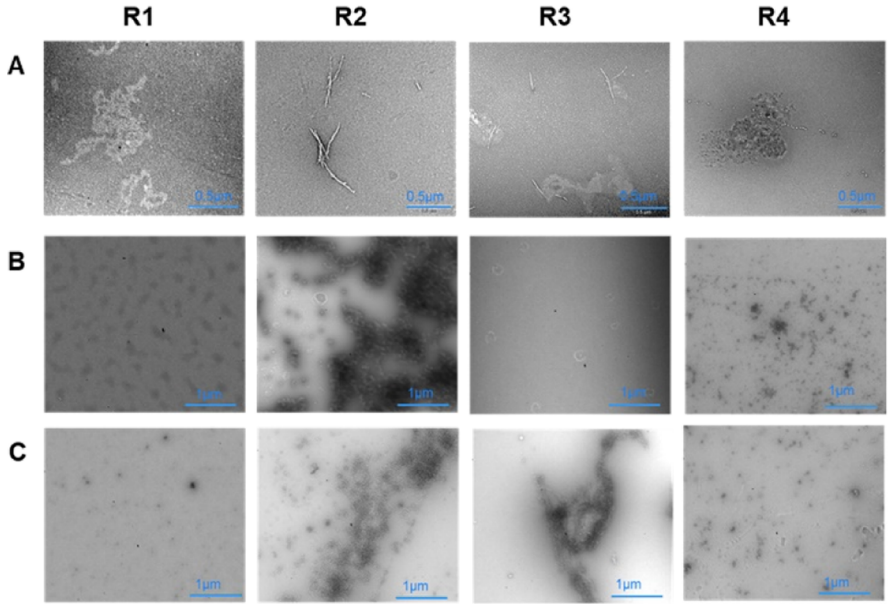

Figure 5. Negative-stain TEM images confirm the influence of Cu^{2+} on the aggregation of MT binding repeats R1−R4. Representative TEM images of R1−R4 after incubation at 25 °C (pH 7.4) for 4 days in (A) Cu^{2+} solution (molar ratio of 2:1 for Cu/R), (B) in AA and Cu^{2+} solution (molar ratio of 20:2:1 for AA/Cu/R), and (C) H_2O_2 solution (molar ratio of 2:1 for H_2O_2/R). (See the Supporting Information for the details) TEM images illustrate the different aggregation profiles of MT binding repeats in oxidative and reducing environments and the presence of amorphous aggregates for R1 and R4 after 4 days incubation in Cu^{2+} solution and formation of fibrils and protofibrils for R2 and R3, respectively, show the impact of Cu^{2+} on R1−R4 aggregation. The observation of amorphous aggregates and oligomers in a reducing environment in the presence of Cu^{2+} reinforces the catalytic role of Cu^{2+} in R1−R4 aggregation.

of R1 with that of the R1−Cu complex (Figures S20 and S21) indicates that these two molecules have a different CCS, which suggests that the R1−Cu complex is more folded. For R4 and its Cu complex, the difference in drift time is significantly less, suggesting that Cu^{2+} has less impact on the conformational changes of R4 (Figures S28 and S29) compared to R1.

Circular dichroism (CD) spectroscopy (Figure S30) showed that all four MT binding repeats mainly have a random coil

DOI: 10.1021/acsomega.8b03595
ACS Omega 2019, 4, 5356−5366

structure, which remains unchanged after 24 h at room temperature. However, the enhancement of the CD signal at 226.7 nm is pointed to the increasing of the α-helix structure in R1 and the negative peak at 294.5 nm indicates the formation of a tertiary structure after incubation of Cu^{2+} for 24 h (Figure S30A). The changes in the CD spectrum of R4 after incubation in Cu^{2+} solution showed a similar trend as R1, but they were less significant (Figure S30D). These observations indicate that the metalation of R1 and R4 leads to conformational and structural changes, which is the first stage of peptide aggregation. The aggregation of MT binding repeats upon Cu^{2+} interaction was also determined by their diffusion coefficients measured using diffusion-ordered spectroscopy (DOSY) NMR spectroscopy. The diffusion data analysis is shown in Figure 4. While no significant changes are observed in the diffusion for R1 and R4 (Figure 4A,D) in the presence of Cu^{2+} (1:1 molar), a considerable decrease in diffusion was detected after the interaction of Cu^{2+} with R2 and R3 (Figure 4B,C). We interpret these differences to be a direct consequence of the aggregation under the reaction conditions.

Our study provides solid evidence that aggregation of the MT binding repeats occurs in the presence of Cu^{2+} ions. We further investigated this influence by studying the morphology of MT binding repeats in the presence and absence of Cu^{2+} ions after 3 and 4 days utilizing transmission electron microscopy (TEM). Based on the ESI-MS results, which show the dimerization of R2 and R3 upon copper interactions, we expected a significant difference between R1−R4 and R2/R3 in the structure of the aggregates. TEM images of R1−R4 in the absence of Cu^{2+} serve as controls and do not show major aggregation (Figures S31 and S32). Incubation of all four MT binding repeats in Cu^{2+} solution led to peptide aggregation after 3 days (Figures S33 and S34). Figure 5 shows a set of representative TEM images of peptides R1−R4 after 4 days of incubation. The R1 showed oligomeric aggregates after 3 days (Figure S33), with the subsequent formation of larger amorphous aggregates (with a maximum size 0.5 × 0.9 μm) after 4 days of incubation in Cu^{2+} solution at room temperature (Figure 5). The R4 also formed oligomeric aggregates in 3 days (Figure S34) and amorphous aggregates after 4 days incubation in Cu^{2+} solution (Figure 5, with a maximum size 0.5 × 0.9 μm). Interestingly, the TEM images indicate that Cu^{2+} mediates the formation of fibrils of R2 and R3. The R2 fibrils started to form together with amorphous aggregates after 3 days incubating in Cu^{2+} solution (Figure S33). The number of fibrils increased dramatically after 4 days (Figure 5, with a maximum length of 1 μm and thickness of 0.02 μm). The Cu^{2+} ions also triggered the aggregation in R3, which led to the formation of amorphous aggregates in 3 days (Figure S34) and protofibrils after 4 days of incubation (Figure 5, with a maximum length of 0.5 μm and thickness of 0.02 μm). While the interaction of Cu^{2+} with R3 produces more ROS, the interaction of Cu^{2+} with R2 leads to more pronounced aggregation.

These experiments confirmed that the peptide aggregation is a consequence of conformational changes and misfolding, which was observed after 24 h incubation of MT binding repeats in Cu^{2+} solution. It also depicted that the dimers can be the seeds for fibril formation. The dramatic differences between peptide with cysteine residues and those without cysteine emphasized the role of cysteine residues in peptide aggregation in the presence of a redox-active metals such as Cu^{2+}.

The R2/R3 aggregation after incubating in Cu^{2+} (molar ratio 2:1 of Cu/R) for 4 days were also evaluated by dynamic light scattering (DLS). A large polydispersity index of 0.76 for R2 suggested that the sample contains large aggregates, which is in agreement with the TEM image that shows the formation of the fibrils. The size distribution plot (Figure S35) shows the presence of three species with the size of 2.5 ± 0.1, 342 ± 32, and 4518 ± 233 nm. The DLS results confirm that the sample mainly contains dimers and remaining are oligomers or fibrils with the molecular weight of 5.7 ± 1.2 × 10^5 and 2.4 ± 0.3 × 10^8 (Table S2). The size distribution plot for R3 (Figure S36) also shows the presence of three species with the size of 3.2 ± 0.1, 220 ± 55, and 1003 ± 662. The R3 sample mainly contains trimers and remaining oligomers with the molecular weight of 2.2 ± 0.8 × 10^7 and 8.8 ± 3.2 × 10^6 (Table S3).

In order to evaluate the formation of the β-sheet upon Cu^{2+} addition, we performed thioflavin-T (ThT) fluorescence experiments. ThT is a common fluorescence probe for monitoring the β-sheet structure.[61−63] It has been shown that the tau protein can adopt a β-sheet structure in the presence of heparin, which was monitored by ThT fluorescence experiments.[33,64] Ganguly et al. studied the self-assembly of the tau fragment R2/wt (273-284) and R3/wt (306-317) and reported the aggregation of R3/wt in the presence of heparin. In addition, while R3/wt displayed a strong ThT fluorescence, the corresponding experiments with R2/wt did not, suggesting potential structural differences. The ThT fluorescence intensity is significantly less for both peptides in the absence of heparin.[64] Figure S37 shows the results of ThT fluorescence experiments for R1−R4 and after 4 days incubation at room temperature in the presence and absence of Cu^{2+}. The results do not allow us to draw any firm conclusion with regard to the internal structure of the aggregates, and one may only speculate that the aggregates exists mainly in the random coil structure.

Our findings suggest the involvement of Cu^{2+} in various steps of the aggregation pathway, which emphasizes the role of Cu^{2+} in AD pathology. We also compared the aggregation profile of peptides R1−R4 in the presence of H_2O_2 as an oxidizing agent. As expected from gel electrophoresis results, the aggregation is more severe in the presence of Cu^{2+} (Figure 5) compared to H_2O_2. The impact of Cu^{2+} on the aggregation of MT binding repeats in a reducing environment was also evaluated by incubation of R1−R4 and Cu^{2+} in the presence of excess AA (1:20:2 molar ratio of R/AA/Cu^{2+}) (Figure 5C). The TEM images show aggregate formation in the presence of Cu^{2+} even under reducing conditions (Figure 2E).

Impact of Glutathione on the Interaction of Cu^{2+} with MT Binding Repeats. Glutathione (GSH) is one of the most abundant nonprotein thiol-containing antioxidants in the neurons, which plays an important role in neutralizing free radicals and reduces the oxidative stress.[65−67] At a healthy brain concentration of GSH is 1−4 mM, which is reduced by age, and as some evidence showed, GSH may be indirectly related to the AD.[65−67] GSH can reduce Cu^{2+} to Cu^{+} with a similar mechanism of R2/R3 by the formation of a disulfide bond, and evidence shows that generated Cu^{+} can bond to GSH.[67−69] However, Speisky et al. showed that the Cu(I)−$[GSH]_2$ complex can reduce the molecular oxygen to superoxide anions.[68,69]

Therefore, we designed a series of experiments to evaluate the impact of GSH on the interaction of Cu^{2+} with MT binding repeats. Because GSH has a high affinity to react with

DOI: 10.1021/acsomega.8b03595
ACS Omega 2019, 4, 5356−5366

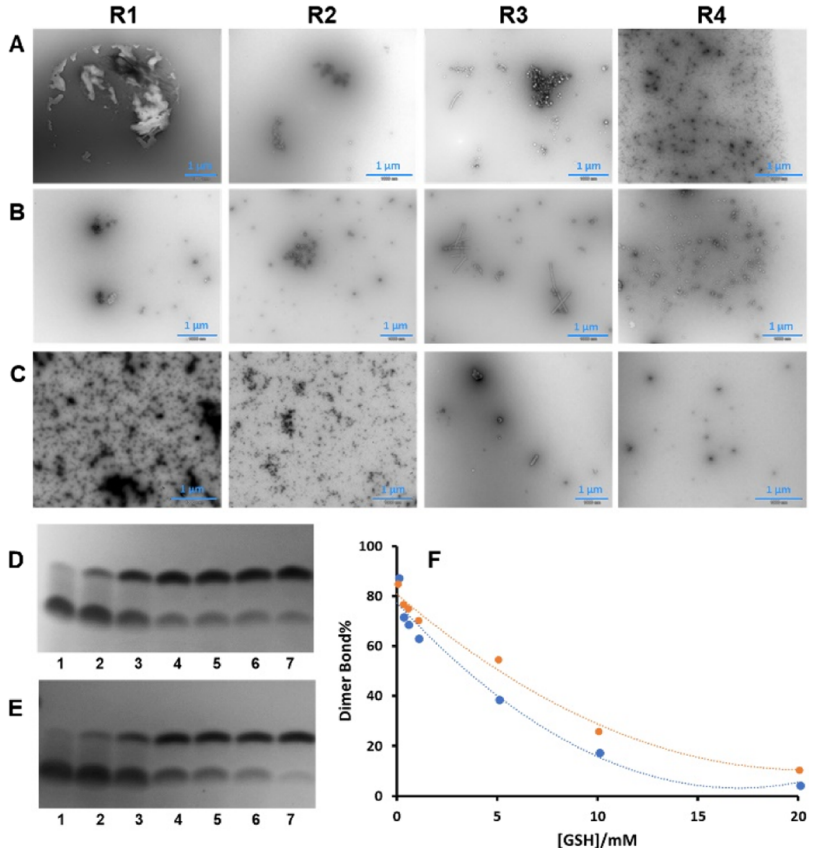

Figure 6. Negative-stain TEM images and gel electrophoresis confirm the influence of Cu^{2+} on the aggregation of MT binding repeats R1−R4 in the presence of glutathione (GSH) and AA. Representative TEM images of R1−R4 after incubation at 25 °C (pH 7.4) for 4 days in (A) Cu^{2+} and GSH (molar ratio of 1:2:1 for R/Cu/GSH) in limited access of oxygen, (B) Cu^{2+} and GSH (molar ratio of 1:0.5:10 for R/Cu/GSH) in ambient oxygen and (C) Cu^{2+}, AA, and GSH (molar ratio of 1:0.5:10:10 for R/Cu/GSH/AA) in ambient oxygen (see the Supporting Information for the details). TEM images illustrate the different aggregation profiles of MT binding repeats in different reducing environments. Formation of amorphous aggregates, oligomers, and protofibrils upon interaction of Cu^{2+} with MT binding repeats in the presence of GSH at various environments suggested that GSH not only does not inhibit the interaction of Cu^{2+} with MT binding repeats but also triggers the MT binding repeat aggregation in particular for R3. Gel electrophoresis of (D) 1 mM R2 and (E) 1 mM R3 after incubation in 0.5 mM Cu^{2+} and (1) 20, (2) 10, (3) 5, (4) 1, (5) 0.5, (6) 0.25 mM GSH, and (7) without GSH at limited access to oxygen. (F) Quantification of gel electrophoresis results; plot of percentage of dimers bonds for R2 (red) and R3 (blue) versus concentration of GSH. The results show that Cu^{2+} triggers the R2/R3 dimerization even in the millimolar concentration of GSH.

the Cu^{2+}, we incubated MT binding repeats (R1−R4) in Cu^{2+} in the presence of GSH (molar ratio of 1:2:1 for R/Cu/GSH) in limited access of oxygen by purging the N_2 in solutions. TEM images (Figures 6A and S38) show that even in the presence of 1 mM GSH, aggregation of MT binding repeats happens, suggesting that Cu^{2+} may have more affinity to interact with MT binding repeats or this interaction is kinetically or thermodynamically more favorable.

The aggregation of MT binding repeats was also evaluated in ambient oxygen at catalytical concentration of Cu^{2+} and high concentration of GSH (molar ratio of 1:0.5:10 for R/Cu/GSH). The TEM images (Figures 6B and S39) confirm the impact of Cu^{2+} on the MT binding repeat aggregation in the presence of 10 mM GSH. Interestingly, more protofibrils in a noticeably larger size were formed for R3 in the presence of higher concentration of GSH and lower concentration of Cu^{2+}, which may suggest a significant role of GSH in R3 aggregation in the presence of Cu^{2+}. These results reinforce the formation of superoxide by Cu(I)−$[GSH]_2$, which is proposed by Speisky et al.[68,69] In order to evaluate the aggregation effect of Cu^{2+} in a strong reducing environment, MT binding repeats were also incubated in Cu^{2+} in the presence of 10 mM GSH and 10 mM AA (molar ratio of 1:0.5:10:10 for R/Cu/GSH/AA) to provide a complex reducing environment.

The TEM images (Figures 6C and S40) show that AA/GSH can reduce the aggregation but cannot completely inhibit the aggregation effect of Cu^{2+}. The inhibitor effect of GSH in preventing the R2 and R3 dimerization, as the first step of aggregation, was evaluated by gel electrophoresis (Figure 6D−F). The R2/R3 (1 mM) dimerization upon the Cu^{2+} (0.5 mM) interaction was monitored in the presence of GSH (0.25−20 mM) and in the limited access of oxygen. The gel electrophoresis shows that at 1 mM concentration of GSH, more than 70% of R2 and 60% of R3 were dimerized. Notably, by increasing the concentration of GSH, a range of peptides with molecular weight between R2/R3 monomers and dimers formed, which may suggest that GSH can bond to the R2/R3 monomer in different molar ratios to form these peptides. These peptides can be seeds for formation of protofibrils, which were observed by TEM. These observations reinforce the key role of Cu^{2+} in the MT binding repeats even in the presence of natural defense of neurons.

DOI: 10.1021/acsomega.8b03595
ACS Omega 2019, 4, 5356−5366

CONCLUSIONS

In the current study, new insight into the interactions of MT binding repeats of the tau protein with Cu^{2+} is provided. One of the finding concerns MT repeats R2 and R3, where it was demonstrated that Cys-based oxidation leading to disulfide bond formation occurs in the presence of Cu^{2+}, with significant consequences to the R2 and R3 fibrillization and ROS formation. Our results unequivocally confirm (a) Cu^{2+} coordination to His268 of R1 and His363 of R4, (b) the dimerization of R2 and R3 via disulfide bond formation, and (c) Cu^{2+} coordination to the R2/R3 dimers. We have no evidence to suggest the formation of stable complexes involving Cys-coordination as reported before for the shorter motif of R2.[21] It is evident that Cu^{2+} is involved in different stages of aggregation by triggering conformational changes of MT binding repeats, the dimerization of R2 and R3, the formation of amorphous aggregates for R1 and R4, and the fibrillization for R2 and R3. These findings are significant within a biological context as they not only are related to differences in the aggregation process of MT binding repeats but also address the role of Cu^{2+} in producing small toxic aggregates that may contribute in neuron death. Our findings also provide a solid evidence for the ROS formation as a result of the redox chemistry exhibited by Cys291 and Cys322 in the presence of Cu^{2+}. Cysteine oxidation in R2 and R3 to the corresponding disulfides occurs even in the presence of glutathione and ascorbate, abundant antioxidants in the neurons. Unusual ROS formation due to the catalytic role of R−Cu adds to the oxidative stress and to cell damage. These experimental findings are significant as they draw a connection between Cu dyshomeostasis under pathological conditions and aggregation of tau and ROS formation inside the neurons as well as CSF.

Our results further support the metal chelators as potential therapeutic agents for AD. In our opinion, preventing Cys-based redox chemistry may be a valuable therapeutic target. Design of molecules with multifunctional activity that not only inhibit tau aggregation by targeting the Cys regions but also chelate the copper to prevent the Cys-based redox chemistry and ROS formation can be more efficient.

EXPERIMENTAL SECTION

All chemicals and reagents were of analytical grade and obtained from Sigma Aldrich. Lipoic acid *N*-hydroxy succinimide ester (Lip−NHS) was synthesized as reported before.[70] Tau Peptide (244-274) (Repeat 1 domain, R1), Tau Peptide (275-305) (Repeat 2 domain, R2), Tau Peptide (306-336) (Repeat 3 domain, R3), and Tau Peptide (337-368) (Repeat 4 domain, R4) were purchased from Anaspec (Fremont, CA, USA). The masses and the purity of the peptides were confirmed by ESI-MS and HPLC (≥95%), respectively. See Scheme 1 for the amino acid sequence of R1−R4. All the chemicals used for gel electrophoresis were purchased from Bio-Rad Laboratories (Canada) Ltd. Millipore-Q water (18.2 MΩ cm) was used for sample preparation, and all the experiments were performed at room temperature and pH 7.4 unless otherwise mentioned. A 10 mM $CuCl_2$ stock solution was prepared in Millipore-Q water right before each experiment and diluted in phosphate buffer, pH 7.4 to the desired concentration. The peptide stock solutions were prepared by dissolving 1 mg of each peptide in Millipore-Q water to get a final concentration of 3 mM. The stock solutions were aliquoted and kept at −20 °C. The $CuCl_2$ solution was added to the peptide with the molar ratio 2:1 of Cu^{2+}/R to shift the equilibrium to the formation of the copper complex unless otherwise mentioned. All the samples were kept at room temperature for 24 h before the experiment unless otherwise mentioned. The details of each experiment are provided in the Supporting Information.

ASSOCIATED CONTENT

Supporting Information

The Supporting Information is available free of charge on the ACS Publications website at DOI: 10.1021/acsomega.8b03595.

Material and methods, mass spectrometry, NMR spectroscopy, UV-visible studies, fluorescence studies, circular dichroism (CD) spectroscopy, electrochemical experiments, transmission electron microscopy experiment, electron paramagnetic resonance (EPR) spectroscopy, isothermal titration calorimetry (ITC), gel electrophoresis, dynamic light scattering, ESI-MS spectra, time-dependent study of the formation of reactive oxygen species, $_1$H NMR spectra, X-band EPR spectra, IMS-MS Driftscope plots, drift time distribution, CD spectra, and TEM images (PDF)

AUTHOR INFORMATION

Corresponding Authors

*E-mail: dkwilson@yorku.ca (D.J.W.).
*E-mail: andre.simpson@utoronto.ca (A.J.S.).
*E-mail: bernie.kraatz@utoronto.ca (H.-B.K.).

ORCID

Bing Wu: 0000-0002-2739-5124
Ronald Soong: 0000-0002-8223-9028
R. Dutta Majumdar: 0000-0001-9232-7331
Derek J. Wilson: 0000-0002-7012-6085
Andre J. Simpson: 0000-0002-8247-5450
Heinz-Bernhard Kraatz: 0000-0002-7149-0110

Present Addresses

⊥Dutch-Belgian Beamline (DUBBLE), ESRF—The European Synchrotron Radiation Facility, CS 40220, 38043 Grenoble Cedex 9, France.
#Bruker Ltd., 2800 High Point Drive, Suite 2016, Milton, ON, Canada.

Author Contributions

All authors have given approval to the final version of the manuscript.

Funding

This project was financial supported by The Natural Sciences and Engineering Research Council of Canada (NSERC, RGPIN-2016-06122).

Notes

The authors declare no competing financial interest.

ACKNOWLEDGMENTS

The authors gratefully acknowledge support from the Natural Science and Engineering Research Council of Canada. In addition, they thank York University's Centre for Research in Mass Spectrometry, UTSC Environmental NMR Centre, Department of Chemistry University of Toronto, and the University of Toronto Scarborough. The Authors also

DOI: 10.1021/acsomega.8b03595
ACS Omega 2019, 4, 5356−5366

acknowledge Dr. Sergiy Nokhrin for help with EPR experiment, Robert Temkin for help with TEM experiments, and Chai Chen for help with gel electrophoresis experiments.

REFERENCES

(1) Wang, Y.; Mandelkow, E. Tau in Physiology and Pathology. *Nat. Rev. Neurosci.* **2016**, *17*, 22−35.
(2) Elie, A.; Prezel, E.; Guérin, C.; Denarier, E.; Ramirez-Rios, S.; Serre, L.; Andrieux, A.; Fourest-Lieuvin, A.; Blanchoin, L.; Arnal, I. Tau Co-Organizes Dynamic Microtubule and Actin Networks. *Sci. Rep.* **2015**, *5*, 9964.
(3) Iqbal, K.; Liu, F.; Gong, C.-X. Tau and Neurodegenerative Disease: The Story so Far. *Nat. Rev. Neurol.* **2016**, *12*, 15−27.
(4) Guo, T.; Noble, W.; Hanger, D. P. Roles of Tau Protein in Health and Disease. *Acta Neuropathol.* **2017**, *133*, 665−704.
(5) Raskatov, J. A.; Teplow, D. B. Using Chirality to Probe the Conformational Dynamics and Assembly of Intrinsically Disordered Amyloid Proteins. *Sci. Rep.* **2017**, *7*, 12433.
(6) Jahn, T. R.; Radford, S. E. The Yin and Yang of Protein Folding. *FEBS J.* **2005**, *272*, 5962−5970.
(7) Ross, C. A.; Poirier, M. A. Protein Aggregation and Neurodegenerative Disease. *Nat. Med.* **2004**, *10*, S10−S17.
(8) Ross, C. A.; Poirier, M. A. Opinion: What Is the Role of Protein Aggregation in Neurodegeneration? *Nat. Rev. Mol. Cell Biol.* **2005**, *6*, 891−898.
(9) Lovell, M. A.; Robertson, J. D.; Teesdale, W. J.; Campbell, J. L.; Markesbery, W. R. Copper, Iron and Zinc in Alzheimer's Disease Senile Plaques. *J. Neurol. Sci.* **1998**, *158*, 47−52.
(10) Miller, L. M.; Wang, Q.; Telivala, T. P.; Smith, R. J.; Lanzirotti, A.; Miklossy, J. Synchrotron-Based Infrared and X-Ray Imaging Shows Focalized Accumulation of Cu and Zn Co-Localized with β-Amyloid Deposits in Alzheimer's Disease. *J. Struct. Biol.* **2006**, *155*, 30−37.
(11) Deibel, M. A.; Ehmann, W. D.; Markesbery, W. R. Copper, Iron, and Zinc Imbalances in Severely Degenerated Brain Regions in Alzheimer's Disease: Possible Relation to Oxidative Stress. *J. Neurol. Sci.* **1996**, *143*, 137−142.
(12) Hung, Y. H.; Bush, A. I.; Cherny, R. A. Copper in the Brain and Alzheimer's Disease. *J. Biol. Inorg Chem.* **2010**, *15*, 61−76.
(13) Madsen, E.; Gitlin, J. D. Copper and Iron Disorders of the Brain. *Annu. Rev. Neurosci.* **2007**, *30*, 317−337.
(14) Barnham, K. J.; Bush, A. I. Biological Metals and Metal-Targeting Compounds in Major Neurodegenerative Diseases. *Chem. Soc. Rev.* **2014**, *43*, 6727−6749.
(15) Bush, A. Metals and Neuroscience. *Curr. Opin. Chem. Biol.* **2000**, *4*, 184−191.
(16) Cotruvo, J. A.; Aron, A. T.; Ramos-torres, K. M.; Chang, C. J. Synthetic Fluorescent Probes for Studying Copper in Biological Systems. *Chem. Soc. Rev.* **2015**, *44*, 4400−4414.
(17) Squitti, R.; Barbati, G.; Rossi, L.; Ventriglia, M.; Dal Forno, G.; Cesaretti, S.; Moffa, F.; Caridi, I.; Cassetta, E.; Pasqualetti, P.; et al. Excess of Nonceruloplasmin Serum Copper in AD Correlates with MMSE, CSF β-Amyloid, and h-Tau. *Neurology* **2006**, *67*, 76−82.
(18) Sparks, D. L.; Schreurs, B. G. Trace Amounts of Copper in Water Induce -Amyloid Plaques and Learning Deficits in a Rabbit Model of Alzheimer's Disease. *Proc. Natl. Acad. Sci. U.S.A.* **2003**, *100*, 11065−11069.
(19) Sparks, D. L.; Friedland, R.; Petanceska, S.; Schreurs, B. G.; Shi, J.; Perry, G.; Smith, M. A.; Sharma, A.; Derosa, S.; Ziolkowski, C.; et al. Trace Copper Levels in the Drinking Water, but Not Zinc or Aluminum Influence CNS Alzheimer-like Pathology. *J. Nutr. Health Aging* **2006**, *10*, 247−254.
(20) Zhou, L.-X.; Du, J.-T.; Zeng, Z.-Y.; Wu, W.-H.; Zhao, Y.-F.; Kanazawa, K.; Ishizuka, Y.; Nemoto, T.; Nakanishi, H.; Li, Y.-M. Copper (II) Modulates in Vitro Aggregation of a Tau Peptide. *Peptides* **2007**, *28*, 2229−2234.
(21) Ma, Q.; Li, Y.; Du, J.; Liu, H.; Kanazawa, K.; Nemoto, T.; Nakanishi, H.; Zhao, Y. Copper Binding Properties of a Tau Peptide Associated with Alzheimer's Disease Studied by CD, NMR, and MALDI-TOF MS. *Peptides* **2006**, *27*, 841−849.
(22) Ma, Q.-F.; Li, Y.-M.; Du, J.-T.; Kanazawa, K.; Nemoto, T.; Nakanishi, H.; Zhao, Y.-F. Binding of Copper (II) Ion to an Alzheimer's Tau Peptide as Revealed by MALDI-TOF MS, CD, and NMR. *Biopolymers* **2005**, *79*, 74−85.
(23) Su, X.-Y.; Wu, W.-H.; Huang, Z.-P.; Hu, J.; Lei, P.; Yu, C.-H.; Zhao, Y.-F.; Li, Y.-M. Hydrogen Peroxide Can Be Generated by Tau in the Presence of Cu(II). *Biochem. Biophys. Res. Commun.* **2007**, *358*, 661−665.
(24) Martic, S.; Rains, M. K.; Kraatz, H.-B. Probing Copper/Tau Protein Interactions Electrochemically. *Anal. Biochem.* **2013**, *442*, 130−137.
(25) Soragni, A.; Zambelli, B.; Mukrasch, M. D.; Biernat, J.; Jeganathan, S.; Griesinger, C.; Ciurli, S.; Mandelkow, E.; Zweckstetter, M. Structural Characterization of Binding of Cu (II) to Tau Protein. *Biochemistry* **2008**, *47*, 10841−10851.
(26) von Bergen, M.; Friedhoff, P.; Biernat, J.; Heberle, J.; Mandelkow, E.-M.; Mandelkow, E. Assembly of Tau Protein into Alzheimer Paired Helical Filaments Depends on a Local Sequence Motif (306VQIVYK311) Forming Beta Structure. *Proc. Natl. Acad. Sci. U.S.A.* **2000**, *97*, 5129−5134.
(27) Ganguly, P.; Do, T. D.; Larini, L.; Lapointe, N. E.; Sercel, A. J.; Shade, M. F.; Feinstein, S. C.; Bowers, M. T.; Shea, J.-E. Tau Assembly: The Dominant Role of PHF6 (VQIVYK) in Microtubule Binding Region Repeat R3. *J. Phys. Chem. B* **2015**, *119*, 4582−4593.
(28) Stöhr, J.; Wu, H.; Nick, M.; Wu, Y.; Bhate, M.; Condello, C.; Johnson, N.; Rodgers, J.; Lemmin, T.; Acharya, S.; et al. A 31-Residue Peptide Induces Aggregation of Tau's Microtubule-Binding Region in Cells. *Nat. Chem.* **2017**, *9*, 874−881.
(29) Mukrasch, M. D.; Biernat, J.; Von Bergen, M.; Griesinger, C.; Mandelkow, E.; Zweckstetter, M. Sites of Tau Important for Aggregation Populate β-Structure and Bind to Microtubules and Polyanions. *J. Biol. Chem.* **2005**, *280*, 24978−24986.
(30) Fitzpatrick, A. W. P.; Falcon, B.; He, S.; Murzin, A. G.; Murshudov, G.; Garringer, H. J.; Crowther, R. A.; Ghetti, B.; Goedert, M.; Scheres, S. H. W. Cryo-EM Structures of Tau Filaments from Alzheimer's Disease. *Nature* **2017**, *547*, 185−190.
(31) Falcon, B.; Zhang, W.; Murzin, A. G.; Murshudov, G.; Garringer, H. J.; Vidal, R.; Crowther, R. A.; Ghetti, B.; Scheres, S. H. W.; Goedert, M. Structures of Filaments from Pick's Disease Reveal a Novel Tau Protein Fold. *Nature* **2018**, *561*, 137−140.
(32) Schweers, O.; Mandelkow, E.-M.; Biernat, J.; Caspar, E. Oxidation of Cysteine-322 in the Repeat Domain of Microtubule-Associated Protein T Controls the in Vitro Assembly of Paired Helical Filaments (Alzheimer Disease/Neurofibrillary Tangles). *Proc. Natl. Acad. Sci. U.S.A.* **1995**, *92*, 8463−8467.
(33) Furukawa, Y.; Kaneko, K.; Nukina, N. Tau Protein Assembles into Isoform- and Disulfide-Dependent Polymorphic Fibrils with Distinct Structural Properties. *J. Biol. Chem.* **2011**, *286*, 27236−27246.
(34) Kadavath, H.; Hofele, R. V.; Biernat, J.; Kumar, S.; Tepper, K.; Urlaub, H.; Mandelkow, E.; Zweckstetter, M. Tau Stabilizes Microtubules by Binding at the Interface between Tubulin Heterodimers. *Proc. Natl. Acad. Sci. U.S.A.* **2015**, *112*, 7501−7506.
(35) Ahmadi, S.; Ebralidze, I. I.; She, Z.; Kraatz, H.-B. Electrochemical Studies of Tau Protein-Iron Interactions—Potential Implications for Alzheimer's Disease. *Electrochim. Acta* **2017**, *236*, 384−393.
(36) Ahmadi, S.; Zhu, S.; Sharma, R.; Wilson, D. J.; Kraatz, H.-B. Interaction of Metal Ions with Tau Protein. The Case for a Metal-Mediated Tau Aggregation. *J. Inorg. Biochem.* **2019**, *194*, 44−51.
(37) Walker, S.; Ullman, O.; Stultz, C. M. Using Intramolecular Disulfide Bonds in Tau Protein to Deduce Structural Features of Aggregation-Resistant Conformations. *J. Biol. Chem.* **2012**, *287*, 9591−9600.
(38) Cheignon, C.; Jones, M.; Atrián-Blasco, E.; Kieffer, I.; Faller, P.; Collin, F.; Hureau, C. Identification of Key Structural Features of the Elusive Cu−Aβ Complex That Generates ROS in Alzheimer's Disease. *Chem. Sci.* **2017**, *8*, 5107−5118.

DOI: 10.1021/acsomega.8b03595
ACS Omega 2019, 4, 5356−5366

(39) Sayre, L. M.; Perry, G.; Harris, P. L. R.; Liu, Y.; Schubert, K. A.; Smith, M. A. In Situ Oxidative Catalysis by Neurofibrillary Tangles and Senile Plaques in Alzheimer's Disease. *J. Neurochem.* **2001**, *74*, 270−279.
(40) Jiang, D.; Li, X.; Liu, L.; Yagnik, G. B.; Zhou, F. Reaction Rates and Mechanism of the Ascorbic Acid Oxidation by Molecular Oxygen Facilitated by Cu(II)-Containing Amyloid-Complexes and Aggregates. *J. Phys. Chem. B* **2010**, *114*, 4896−4903.
(41) Ząbek-Adamska, A.; Drożdż, R.; Naskalski, J. W. Dynamics of Reactive Oxygen Species Generation in the Presence of Copper (II)− Histidine Complex and Cysteine. *Acta Biochim. Pol.* **2013**, *60*, 565− 571.
(42) Rastogi, R. P.; Singh, S. P.; Häder, D.-P.; Sinha, R. P. Detection of Reactive Oxygen Species (ROS) by the Oxidant-Sensing Probe 2',7'-Dichlorodihydrofluorescein Diacetate in the Cyanobacterium Anabaena Variabilis PCC 7937. *Biochem. Biophys. Res. Commun.* **2010**, *397*, 603−607.
(43) Chen, X.; Zhong, Z.; Xu, Z.; Chen, L.; Wang, Y. 2′,7′-Dichlorodihydrofluorescein as a Fluorescent Probe for Reactive Oxygen Species Measurement: Forty Years of Application and Controversy. *Free Radical Res.* **2010**, *44*, 587−604.
(44) Gaubert, S.; Bouchaut, M.; Brumas, V.; Berthon, G. Copper-Ligand Interactions and Physiological Free Radical Processes. Part 3. Influence of Histidine, Salicylic Acid and Anthranilic Acid on Copper-Driven Fenton Chemistry in Vitro. *Free Radical Res.* **2000**, *32*, 451− 461.
(45) Shin, B.-K.; Saxena, S. Insight into Potential Cu (II) -Binding Motifs in the Four Pseudorepeats of Tau Protein. *J Phys Chem B* **2011**, *115*, 15067−15078.
(46) De Ricco, R.; Potocki, S.; Kozlowski, H.; Valensin, D. NMR Investigations of Metal Interactions with Unstructured Soluble Protein Domains. *Coord. Chem. Rev.* **2014**, *269*, 1−12.
(47) Gaggelli, E.; D'Amelio, N.; Valensin, D.; Valensin, G. 1H NMR Studies of Copper Binding by Histidine-Containing Peptides. *Magn. Reson. Chem.* **2003**, *41*, 877−883.
(48) Choi, D.; Alshahrani, A. A.; Vytla, Y.; Deeconda, M.; Serna, V. J.; Saenz, R. F.; Angel, L. A. Redox Activity and Multiple Copper(I) Coordination of 2His-2Cys Oligopeptide. *J. Mass Spectrom.* **2015**, *50*, 316−325.
(49) Bae, J.-Y.; Koo, B.-K.; Ryu, H.-B.; Song, J.-A.; Nguyen, M. T.; Vu, T. T. T.; Son, Y.-J.; Lee, H. K.; Choe, H. Cu/Zn Incorporation during Purification of Soluble Human EC-SOD from E. Coli Stabilizes Proper Disulfide Bond Formation. *Appl. Biochem. Biotechnol.* **2013**, *169*, 1633−1647.
(50) Peisach, J.; Blumberg, W. E. Structural Implications Derived from the Analysis of Electron Paramagnetic Resonance Spectra of Natural and Artificial Copper Proteins. *Arch. Biochem. Biophys.* **1974**, *165*, 691−708.
(51) Aronoff-Spencer, E.; Burns, C. S.; Avdievich, N. I.; Gerfen, G. J.; Peisach, J.; Antholine, W. E.; Ball, H. L.; Cohen, F. E.; Prusiner, S. B.; Millhauser, G. L. Identification of the Cu2+ Binding Sites in the N-Terminal Domain of the Prion Protein by EPR and CD Spectroscopy. *Biochemistry* **2000**, *39*, 13760−13771.
(52) Chattopadhyay, M.; Walter, E. D.; Newell, D. J.; Jackson, P. J.; Aronoff-Spencer, E.; Peisach, J.; Gerfen, G. J.; Bennett, B.; Antholine, W. E.; Millhauser, G. L. The Octarepeat Domain of the Prion Protein Binds Cu(II) with Three Distinct Coordination Modes at PH 7.4. *J. Am. Chem. Soc.* **2005**, *127*, 12647−12656.
(53) del Pino, P.; Weiss, A.; Bertsch, U.; Renner, C.; Mentler, M.; Grantner, K.; Fiorino, F.; Meyer-Klaucke, W.; Moroder, L.; Kretzschmar, H. A.; et al. The Configuration of the Cu2+ Binding Region in Full-Length Human Prion Protein. *Eur. Biophys. J.* **2007**, *36*, 239−252.
(54) Gala, L.; Lawson, M.; Jomova, K.; Zelenicky, L.; Congradyova, A.; Mazur, M.; Valko, M. EPR Spectroscopy of a Clinically Active (1:2) Copper(II)-Histidine Complex Used in the Treatment of Menkes Disease: A Fourier Transform Analysis of a Fluid CW-EPR Spectrum. *Molecules* **2014**, *19*, 980−991.
(55) Silva, K. I.; Michael, B. C.; Geib, S. J.; Saxena, S. ESEEM Analysis of Multi-Histidine Cu(II)-Coordination in Model Complexes, Peptides, and Amyloid-*β*. *J. Phys. Chem. B* **2014**, *118*, 8935− 8944.
(56) Shearer, J.; Szalai, V. A. The Amyloid-*β* Peptide of Alzheimer's Disease Binds Cu(I) in a Linear Bis-His Coordination Environment: Insight into a Possible Neuroprotective Mechanism for the Amyloid-*β* Peptide. *J. Am. Chem. Soc.* **2008**, *130*, 17826−17835.
(57) Faller, P.; Hureau, C.; La Penna, G. Metal Ions and Intrinsically Disordered Proteins and Peptides: From Cu/Zn Amyloid-*β* to General Principles. *Acc. Chem. Res.* **2014**, *47*, 2252−2259.
(58) Cereghetti, G. M.; Schweiger, A.; Glockshuber, R.; Van Doorslaer, S. Electron Paramagnetic Resonance Evidence for Binding of Cu2+ to the C-Terminal Domain of the Murine Prion Protein. *Biophys. J.* **2001**, *81*, 516−525.
(59) Bukharov, M. S.; Shtyrlin, V. G.; Mamin, G. V.; Stapf, S.; Mattea, C.; Mukhtarov, A. S.; Serov, N. Y.; Gilyazetdinov, E. M. Structure and Dynamics of Solvation Shells of Copper(II) Complexes with N,O-Containing Ligands. *Inorg. Chem.* **2015**, *54*, 9777−9784.
(60) Sakaguchi, U.; Addison, A. W. Spectroscopic and Redox Studies of Some Copper(II) Complexes with Bio-Mimetic Donor Atoms: Implications for Protein Copper Centres. *J. Chem. Soc., Dalton Trans.* **1979**, 600−608.
(61) Biancalana, M.; Koide, S. Molecular Mechanism of Thioflavin-T Binding to Amyloid Fibrils. *Biochim. Biophys. Acta, Proteins Proteomics* **2010**, *1804*, 1405−1412.
(62) Groenning, M. Binding Mode of Thioflavin T and Other Molecular Probes in the Context of Amyloid Fibrils-Current Status. *J. Chem. Biol.* **2010**, *3*, 1−18.
(63) Xue, C.; Lin, T. Y.; Chang, D.; Guo, Z. Thioflavin T as an Amyloid Dye: Fibril Quantification, Optimal Concentration and Effect on Aggregation. *R. Soc. Open Sci.* **2017**, *4*, 160696.
(64) Ganguly, P.; Do, T. D.; Larini, L.; Lapointe, N. E.; Sercel, A. J.; Shade, M. F.; Feinstein, S. C.; Bowers, M. T.; Shea, J.-E. Tau Assembly: The Dominant Role of PHF6 (VQIVYK) in Microtubule Binding Region Repeat R3. *J. Phys. Chem. B* **2015**, *119*, 4582−4593.
(65) Rae, C. D.; Williams, S. R. Glutathione in the Human Brain: Review of Its Roles and Measurement by Magnetic Resonance Spectroscopy. *Anal. Biochem.* **2017**, *529*, 127−143.
(66) Mandal, P. K.; Saharan, S.; Tripathi, M.; Murari, G. Brain Glutathione Levels − A Novel Biomarker for Mild Cognitive Impairment and Alzheimer ' s Disease. *Biol. Psychiatry* **2015**, *78*, 702−710.
(67) Pocernich, C. B.; Butterfield, D. A. Elevation of Glutathione as a Therapeutic Strategy in Alzheimer Disease. *Biochim. Biophys. Acta* **2012**, *1822*, 625−630.
(68) Speisky, H.; Gómez, M.; Burgos-bravo, F.; López-Alarcón, C.; Jullian, C.; Olea-azar, C.; Aliaga, M. E. Generation of Superoxide Radicals by Copper − Glutathione Complexes: Redox-Consequences Associated with Their Interaction with Reduced Glutathione. *Bioorg. Med. Chem.* **2009**, *17*, 1803−1810.
(69) Speisky, H.; Gómez, M.; Carrasco-Pozo, C.; Pastene, E.; Lopez-Alarcón, C.; Olea-Azar, C. Cu (I)− Glutathione Complex: A Potential Source of Superoxide Radicals Generation. *Bioorg. Med. Chem.* **2008**, *16*, 6568−6574.
(70) Martić, S.; Beheshti, S.; Rains, M. K.; Kraatz, H.-B. Electrochemical Investigations into Tau Protein Phosphorylations. *Analyst* **2012**, *137*, 2042−2046.

DOI: 10.1021/acsomega.8b03595
ACS Omega 2019, 4, 5356−5366